Changes in contact angles as a function of time on some pre-oxidized biomaterials

Y. OSHIDA
Department of Dental Materials, Indiana University School of Dentistry,
1121 W. Michigan St, Indianapolis, IN 46202, USA

R. SACHDEVA
Department of Orthodontics, Baylor College of Dentistry, Dallas, TX 75246, USA

S. MIYAZAKI
Institute of Materials Science, University of Tsukuba, Tsukuba, Ibaraki 305, Japan

Interfaces between biomaterials, tissue and body fluids such as blood play a key role in determining the nature of the interaction between biomaterials and the living organism. The wettability of these biomaterials in relationship to their microenvironment is an important factor to consider when characterizing surface behaviour. The measure of the contact angle between a fluid and material surface can be used to define wettability for that particular microenvironment.

In this study, pure Ti, Ti6Al4V alloy, austenitic and martensitic Ni–Ti alloys, pure Ni, AISI Type 316L stainless steel, Co–Cr alloy, and α-alumina were investigated. All metallic materials were mechanically polished and oxidized at 300 °C for 30 min in pure oxygen. Oxide films formed on the surfaces of these materials were examined under the electron microscope and their crystalline structures were identified by the electron diffraction method. The initial contact angle (θ_0) and its changes ($\delta\theta/\delta t$) as a function of time in 1% NaCl solution drop were measured.

The results of this study indicated that (i) Ti and its alloys were covered with mainly TiO_2 (tetragonal structure), (ii) NiO (cubic structure) was found on pure Ni, (iii) the spinel type oxide (cubic structure) was formed on both 316L stainless steel and Co–Cr alloy, (iv) TiO_2 (except for oxides formed on Ti6Al4V alloy) showed a rapid spreading characteristic in 1% NaCl solution; while (v) a relatively slow spreading behaviour was observed on the cubic structure oxides.

1. Introduction

The interactions which occur at the interface between an implant and a tissue fall clearly into the niche of interdisciplinary fields such as surface chemistry, physics, and surface characterizations [1]. Surface characterizations are very important in the development of blood- or tissue-compatible biomaterials. Surfaces and interfaces can be characterized through various microanalyses including roughness analysis, contact angle measurements, X-ray photoelectron spectroscopy, reflection infrared spectroscopy, auger electron spectroscopy, secondary ion mass spectroscopy, and/or scanning or transmission electron microscopy [2, 3]. Furthermore, structural analyses by using X-ray or electron diffraction technique should be included.

The wettability of biological materials by liquids and biological fluids is governed by the relative magnitudes of the intermolecular forces between the solid and the liquid [4]. One parameter which characterizes the wettability of a solid is the angle of contact (θ). The angle formed between a solid surface to a normal

direction at the liquid contacting periphery can be measured and defined as a contact angle. Although the contact angle measurement technique is a simple one, it has been recognized that the relationship between contact angle data and surface structure is always inferential and is highly dependent upon extreme surface orientation [5].

If surface tension acting on solid, liquid, solid–liquid interfaces are balanced, it is said that thermodynamic equilibrium exists between the liquid and solid surfaces [6]. However, if the surface is previously wetted [6], the surface roughness is increased [7], or oxidation is involved in surface reaction [8], there is a contact angle hysteresis. Also it was reported that the wettability is time dependent with a tendency to progress from the hydrophobic to the hydrophilic state [9].

All types of metallic biomaterials are covered with a thin oxide film. These might either be air-formed oxides or oxidized films formed by, for instance, sterilization treatment. Hence, surface wettability characteristics should be correlated with both the crystalline

structure and chemical composition of the surface oxide films. As discussed earlier, surface layers of biomaterials may be characterized by measuring contact angle, which can serve as an important measure for evaluating wettability.

The object of the present studies was (i) to analyse the crystalline structures of surface layers of various types of biomaterials, and (ii) to correlate the contact angles with their particular surface oxide structures.

2. Test materials and experimental procedures

All together eight samples were prepared for this study. These included (1) pure titanium, (2) Ti6Al4V alloy, (3) Ti–50 at % Ni (martensite phase, having $M_s \sim +50\,°C$), (4) Ti–51 at % Ni (austenite phase, having $M_s \sim 0\,°C$), (5) AISI Type 316L stainless steel, (6) Co–Cr alloy (27% Cr, 2.0% Ni, 5% Mo, balance Co), (7) pure nickel, and (8) α-Al_2O_3. A specific temperature "M_s" is called a martensitic transformation (from an austenitic phase) start temperature.

Each test coupon had a dimension of 25 mm $\times$ 25 mm $\times$ 2 mm. Surfaces of metallic test coupons were mechanically polished with metallographic papers (grit no. 600). All metallic test coupons were then oxidized in pure oxygen at 300 °C for 30 min. Although the temperature of this pre-oxidation condition was higher than the normally used sterilization temperature (i.e. 100–150 °C), a 300 °C oxidizing temperature was used in these studies to ensure a uniform thin oxide film on the surfaces of various test coupons. Oxide films formed on the mechanically polished surfaces were then stripped by using a well-developed "bromine–ethanol technique" [10]. The stripped oxide films were observed under transmission electron microscope (TEM) and were subject to transmission electron diffraction (TED) at a 120 kV accelerating voltage, to identify the crystalline structures of formed oxides.

Pre-oxidized surfaces of the mechanically polished surfaces were then subject to contact angle measurements by using the sessile drop method [11] using 1% NaCl aqueous solution. The contact angles (θ) can be obtained by the following Equation 1 (see Fig. 1):

$$\theta = 2\tan^{-1}(2h/d) \qquad (1)$$

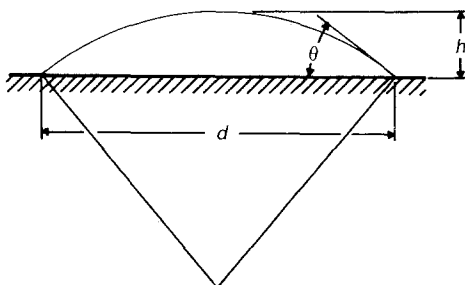As time goes on, h decreases, both due to partial

evaporation of the drop and spreading at the contacting peripheries, and d increases due to the spreading/wetting process. Both factors result in a decrease in the contact angle θ. Therefore, it is required to differentiate θ with respect to time t:

$$\delta\theta/\delta t = \{-4h(\delta d/\delta t) + 4d(\delta h/\delta t)\}/(d^2 + 4h^2) \qquad (2)$$

The term $\delta h/\delta t$ can be referred as to a time-dependent spreading coefficient.

3. Results and discussion
3.1. Microstructure and crystalline structure of oxide films

Figs 2–8 show transmission electron micrographs ($\times 32500$) of stripped oxide films formed on mechanically polished surfaces of all test coupons after being oxidized at 300 °C for 30 min in pure oxygen. Oxide films formed on both pure Ti (Fig. 2) and Ti6Al4V alloy (Fig. 3) showed similarly smooth and uniform microstructures. It was calculated that the average grain size of oxides formed on both Ti and Ti alloy was approximately 20 nm.

As shown in Figs 4 and 5, oxide films formed on both types of Ni–Ti alloys showed agglomerates of single oxide crystals, whose average size was about 15–20 nm. Oxide films formed on 316L type stainless steel (Fig. 6), Co–Cr alloy (Fig. 7) and pure nickel (Fig. 8) show similar uniform oxide layers with island-like agglomerates of oxides, whose size is approximately 10–15 nm.

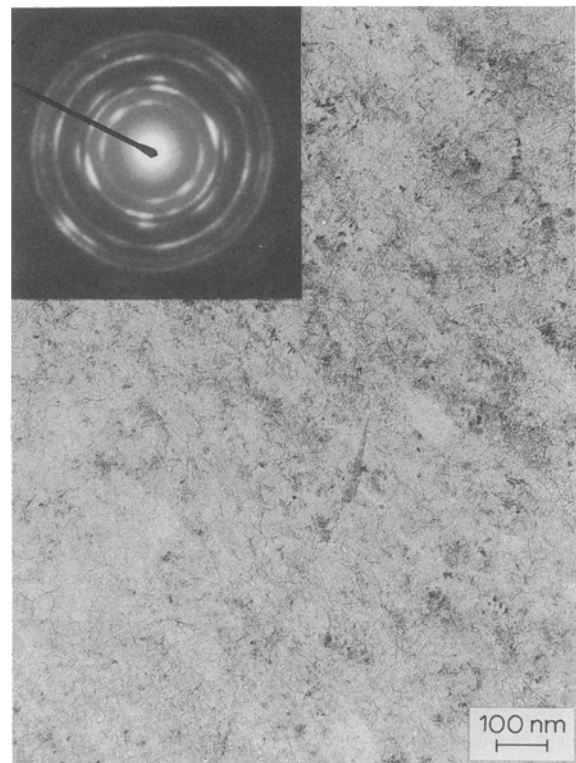TED patterns are also shown on each of the electron micrographs. By using Pt foil as a reference

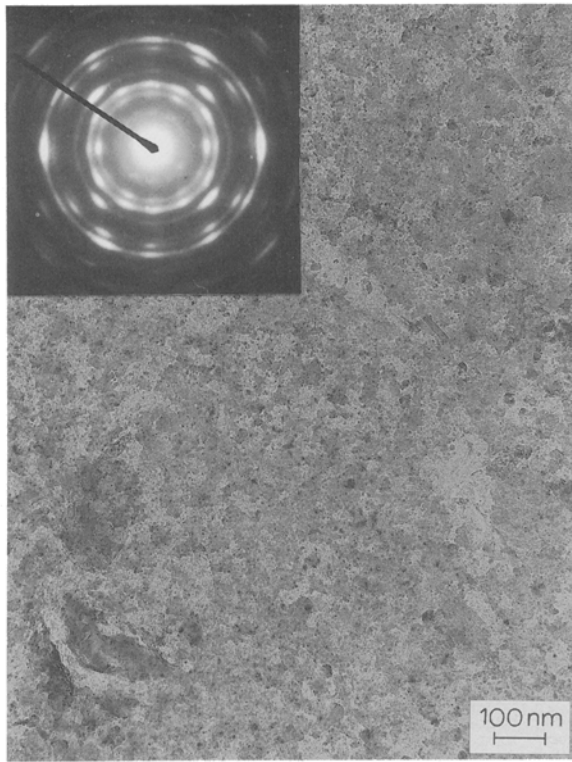*Figure 2* Microstructure and diffraction pattern of oxides formed on pure titanium.

Figure 1 Contact angle measurement. $\theta = 2\tan^{-1}(2h/d)$.

Figure 3 Microstructure and diffraction pattern of oxides formed on Ti6Al4V.
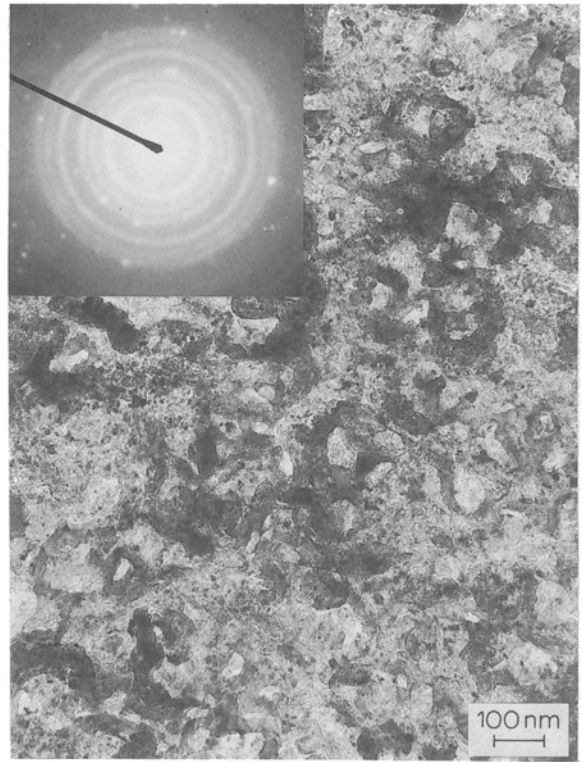

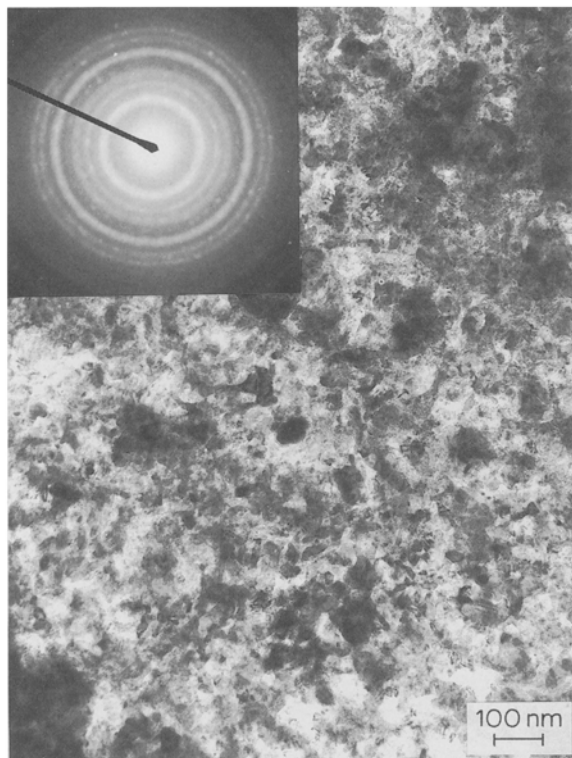*Figure 5* Microstructure and diffraction pattern of oxides formed on Ni–Ti (a).

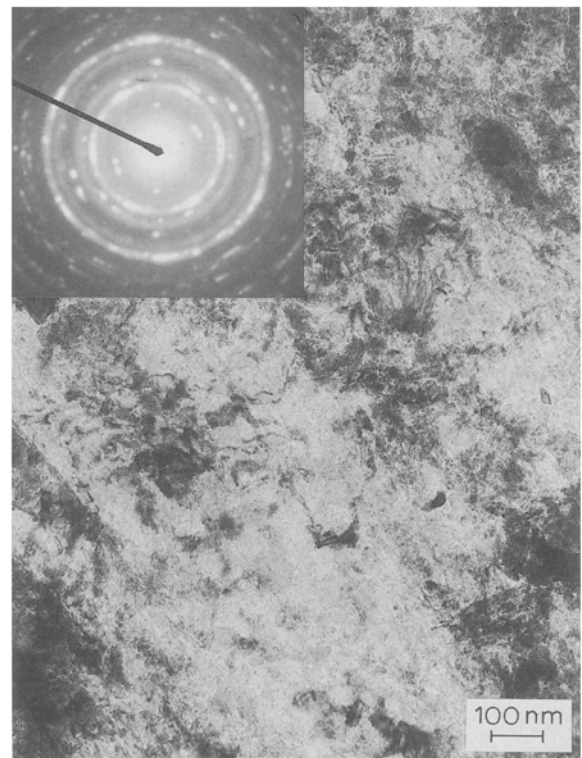*Figure 4* Microstructure and diffraction pattern of oxides formed on Ni–Ti (m).

Figure 6 Microstructure and diffraction pattern of oxides formed on 316L stainless steel.

sample and keeping the same accelerating voltage for the electron diffraction, one can calculate the d-spacings of each oxide film by using $2rd_{sample} = 2rd_{Pt}$, where r is the measured radius of diffracted rings, and d_{sample} is the lattice spacing of each crystalline index, with d_{Pt} (d-spacings of Pt foil) being known.

The oxide film formed on pure Ti was identified as TiO_2 (rutile). A TiO_2 with trace amount of Al_2TiO_5 was formed on Ti6Al4V alloy. It was further observed that surfaces of both the martensitic and austenitic phases of Ni–Ti alloys were covered with a mixture of TiO_2 and $NiTiO_3$. On the other hand, oxide film
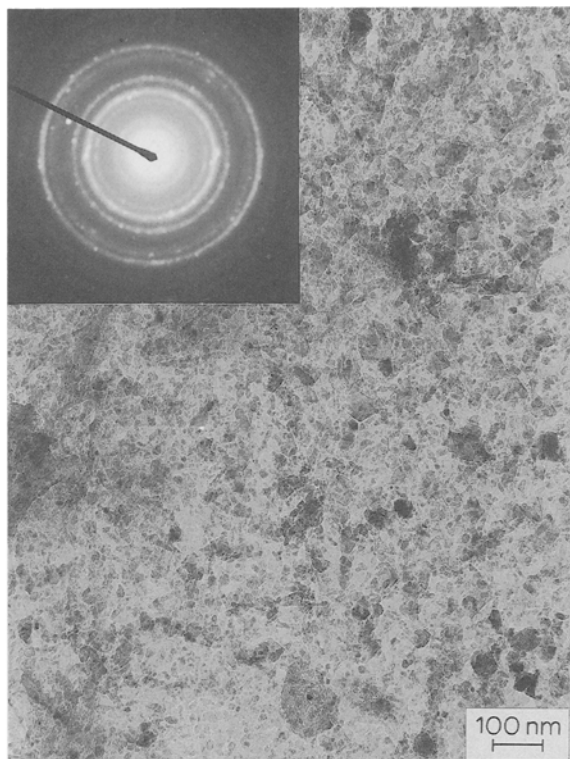
Figure 7 Microstructure and diffraction pattern of oxides formed on Co–Cr alloy.
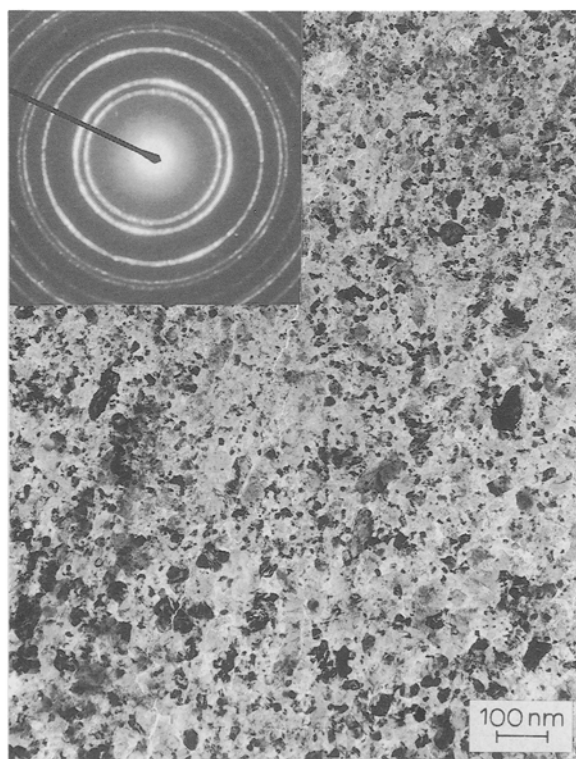

Figure 8 Microstructure and diffraction pattern of oxides formed on pure nickel.

formed on 316L stainless steel was identified as a mixture of spinel-type oxide and corundum-type oxide. According to Oshida *et al.* [10], the spinel-type oxide may be (Fe, Ni)O · (Fe, Cr)$_2$O$_3$ while the corundum-type oxide could be (Fe, Cr)$_2$O$_3$. It was found
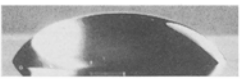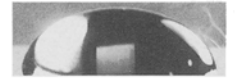
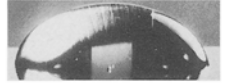*Figure 9* Initial contact angles measured on pre-oxidized mechanically polished biomaterials.

that Co–Cr alloy was covered with pure CoCr$_2$O$_4$ (spinel-type oxide). Finally, the oxide film formed on pure nickel was identified as NiO (cubic structure).

In summary, oxide films formed on Ti and Ti-based alloys (Ti6Al4V, Ni–Ti alloys) consisted mainly of TiO$_2$ (rutile); while oxide films formed on 316L and Co–Cr alloy was spinel-type (plus corundum-type) oxide and NiO was formed on pure nickel. It is known that TiO$_2$ has a tetragonal crystal system; while the spinel type oxide is (face-centred) cubic, and NiO has a NaCl-type cubic structure [12].

3.2. Contact angles of biomaterials

For all materials studied, both initial and changes in contact angles as a function of time were measured three times. Experimental results shown are average values of the three readings. In this study, effect of pre-wetted surfaces on succeeding contact angle measurements was not studied. The standard deviation for the averaged contact angle measurements was between ± 3.0 and ± 5.0 in degrees.

Fig. 9 shows the initial contact angles (θ_0) for the pre-oxidized surfaces of mechanically polished biomaterials when using 1% NaCl aqueous solution drop. Fig. 10 shows the changes in contact angles of the mechanically polished and oxidized surfaces as a function of time. The initial contact angle (θ_0) and the negative slope of change of the contact angle ($\delta\theta/\delta t$) for all tested materials are listed in Table I. It is of interest to investigate how fast a droplet can spread over the surfaces of different biomaterials. Therefore, results in $\delta\theta/\delta t$ are from a non-equilibrium state, and should be understood as purely empirical.

From Table I and Fig. 10, mechanically polished surfaces of tested biomaterials can be classified into three groups: (i) low initial contact angle (θ_0) with low $\delta\theta/\delta t$ for pure nickel and Ti6Al4V alloy; (ii) high θ_0

309

TABLE I Initial contact angles and changes in contact angles as a function of time of oxidized surfaces of biomaterials after mechanical and buff polishing

	Mechanical polish–oxidizing		Buff polish–oxidizing	
	θ_0 (deg)	$\delta\theta/\delta t$	θ_0 (deg)	$\delta\theta/\delta t$
Pure Ti	54.24	− 0.0046		
Ti6Al4V	32.08	− 0.0010	30.85	− 0.0015
NiTi(m)	69.88	− 0.0055	68.92	− 0.0053
NiTi (a)	71.79	− 0.0048		
316L s.s.	56.46	− 0.0024	55.73	− 0.0025
Pure Ni	35.72	− 0.0016		
Co–Cr alloy	62.04	− 0.0023	61.85	− 0.0021
α-alumina	60.87	− 0.0044		

with low $\delta\theta/\delta t$ for 316L stainless steel and Co–Cr alloy; and (iii) high θ_0 with high $\delta\theta/\delta t$ for pure Ti, Ni–Ti alloys and an α-alumina.

It was known that increasing surface roughness causes the contact angle hysteresis [7]. Since the film thickness of surface oxide formed by the pre-oxidation (at 300 °C for 30 min in pure oxygen) was relatively thin, the roughness of the mechanically polished surface may be maintained and traced onto the surface oxide roughness. As seen in the upper portion of Fig. 11, scratches formed during a mechanical polishing (by using no. 600 grit metallographic papers) were traced on the oxide surface of AISI Type 316L stainless steel, with several patty-like oxide agglomerates. On the other hand, as shown in the lower portion of Fig. 11, the buff-polished surface (by using 0.03 μm granular α-alumina emulsion) of this material revealed

more smooth surface. After pre-oxidation, the smooth surface was maintained with patty-like oxide agglomerates which are similar structures, as seen in Fig. 6. By using Ti6Al4V and Ni–Ti (martensitic phase, 316L stainless steel, and Co–Cr alloy), the contact angles of both mechanically and buff-polished surfaces were measured. Results of initial contact angle measurements (see Fig. 12) show no differences from previous polishing methods. Differences in θ_0 between mechanically and buff-polished surfaces (followed by pre-oxidation) are within the experimental standard deviation (i.e. ± 3– ± 5 degrees in θ_0). It was also found that the non-equilibrium changes in θ as a function of time, $\delta\theta/\delta t$, was − 0.0015 for Ti6Al4V, − 0.0053 for Ni–Ti (m), − 0.0025 for 316L stainless steel, and − 0.0021 for Co–Cr alloy. Comparing these data with those listed in Table I indicates that differences in surface roughnesses between the mechanical and buff polishing did not show any significant effects on both initial contact angles and changes in contact angle as a function of time.

White [13] and Bewig et al. [14] reported that surfaces of metal oxides are completely wetted by water, indicating that the contact angle θ should become nearly 0°. However, as shown in Fig. 4, α-alumina shows $\theta = 60.87°$. Besides, all surfaces of metallic materials (which are covered with metal oxides) showed that they were not completely wetted by 1% NaCl solution drop; consequently they can be considered to be hydrophobic at initial contact with 1% NaCl solution.

In various works, surface tension (which is a function of an equilibrium contact angle) has been correlated with different physical parameters including atomic volume, elastic modulus, melting points, and
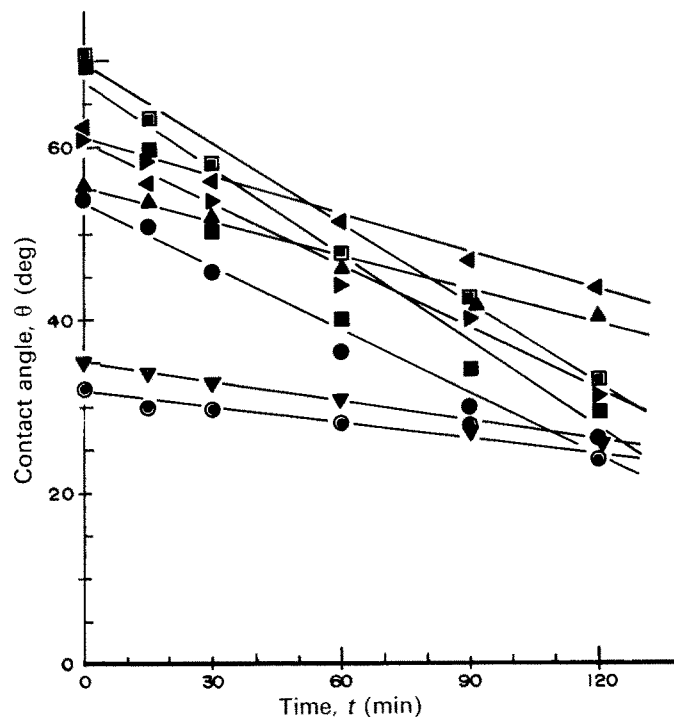

Figure 10 Changes of contact angles versus time, 1% NaCl solution, mechanical polishing to oxidizing at 300 °C for 30 min in pure oxygen. (●) Pure Ti, (◉) Ti6Al4V alloy, (■) Ni–Ti alloy (martensitic phase), (▣) Ni–Ti alloy (austenitic phase), (▲) 316L stainless steel, (▼) pure Ni, (◀) Co–Cr alloy, (▶) α-alumina.
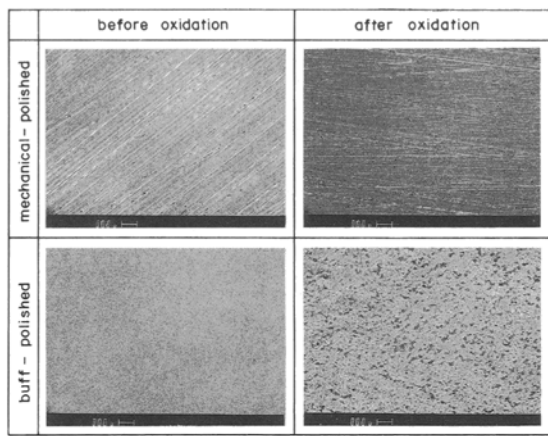
Figure 11 Scanning electron microstructures of mechanical- and buff-polished surfaces of 316L stainless steel before and after pre-oxidation.
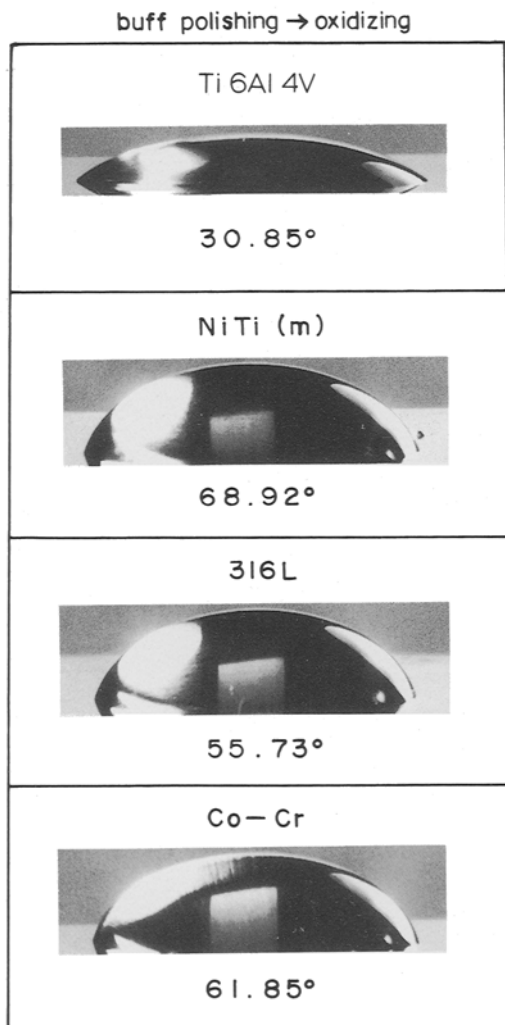
buff polishing → oxidizing

Figure 12 Initial contact angles measured on pre-oxidized buff-polished surfaces.

heat and energy of vaporization [15–17]. Grosse [17] showed a linear relationship between surface tension and heat of vaporization for various pure metals and found that this relationship depends on the crystalline structures (hexagonal structure versus cubic structure) of examined metals. The results obtained from this study indicate also a dependency on crystalline structure of the initial contact angle. To fully understand the effects of crystalline structures on both initial contact angle and its changes as a function of time, further studies are needed, including: (i) grain size effects of oxide films, (ii) crystalline orientation of oxide films and its effects, and (iii) effect of internal stresses generated at oxide film and substrate layer interface.

4. Summary and conclusions

Surfaces of metallic biomaterials which included pure titanium and its alloys (Ti6Al4V, Ti–50 at % Ni, and Ti–51 at % Ni), pure nickel, AISI Type 316L stainless steel, Co–Cr alloy, and α-alumina were studied. Their surfaces were mechanically polished and oxidized in pure oxygen at 300 °C for 30 min. Oxide films formed on the metallic biomaterials were stripped and examined under the electron microscope and identified by electron diffraction techniques. Furthermore, the oxidized surfaces were investigated to characterize their wettability in response to a drop of 1% NaCl solution in terms of contact angle and related time-dependent non-equilibrium phenomena.

Within the limited scope of the experimental study the following conclusions were drawn.

1. The oxide film formed on pure Ti was identified as TiO_2. A mixture of TiO_2 with trace amounts of Al_2TiO_3 was formed on Ti6Al4V alloy, and a mixture of TiO_2 and $NiTiO_3$ was identified on both martensitic and austenitic Ni–Ti alloys. Therefore, all pure Ti and its alloys are mainly covered with a *tetragonal* type TiO_2 (rutile).

2. AISI Type 316L stainless steel was covered with a mixture of spinel-type oxide ($M'O \cdot M_2''O_3$, where M' is Fe^{2+} and Ni^{2+}, and M'' is Fe^{3+} and Cr^{3+}), mixed with a corundum-type oxide ($M_2''O_3$). The surface oxide film formed on Co–Cr alloy was identified as the spinel-type oxide ($CoCr_2O_4$); while NiO was formed on pure nickel. Oxide films formed on 316L stainless steel, Co–Cr alloy and pure nickel show a *cubic* structure.

3. All tested materials showed initial contact angles (θ_0) between 0° and 90°, indicating that they were not completely wetted in 1% NaCl solution. Changes in contact angles as a function of time (for 120 min) indicate that all tested materials may be classified into three groups, (i) low initial contact angle (θ_0) with low $\delta\theta/\delta t$ for pure nickel and Ti6Al4V alloy, (ii) high θ_0 with low $\delta\theta/\delta t$ for 316L stainless and Co–Cr alloy, and (iii) high θ_0 with high $\delta\theta/\delta t$ for pure Ti, Ni–Ti alloys, and α-alumina.

4. It was suggested that the wetting phenomena for all biomaterials (except Ti6Al4V alloy) in 1% NaCl solution seemed to be related to the crystalline structure of the oxide films formed on the surfaces. Namely, TiO_2 oxide responded to high θ_0 with high $\delta\theta/\delta t$ change, and cubic oxides (spinel-type of $M'O \cdot M_2''O_3$ and NiO) showed low $\delta\theta/\delta t$ rates.

References

1. M. N. JONES, in "Biological interfaces" (Elsevier, New York, 1975) pp. 2–3.

311

2. K. H. KELLER, J. D. AADRADE, R. E. BAIER, E. O. DILLINGHAM, J. ELY, F. D. ALTIERI, B.W. MORRISEY and E. KLEIN, National Heart, Lung, Blood Institute, NIH Publ. no. 80–2186 (1980).
3. B. D. RATNER, in "Biomaterials: interfacial phenomena and applications". *Adv. Chem. Ser.* **199** (1982) 9–23.
4. R. E. BAIER, R. C. DUTTON and V. L. GOTT, in "Surface chemistry of biological systems" (Plenum Press, New York, 1970) p. 235.
5. R. J. GOOD, in "Surface and colloid science" (Plenum Press, New York, 1979) p. 1.
6. N. K. ADAM, "The chemical structure of solid surface as deduced contact angles", in "Contact angle: wettability and adhesion", edited by R. F. Gould, *Adv. Chem. Ser.* **43** (1964) 52–56.
7. R. E. JOHNSON Jr and R. H. DETTRE, "Contact angle hysteresis", in "Contact angle: wettability and adhesion", edited by R. F. Gould, *ibid.* **43** (1964) 112–135.
8. A. M. GAUDIN and A. F. WITT, "Hysteresis of contact angles in the system mercury–benzene–water", in "Contact angle: wettability and adhesion", edited by R. F. Gould, *ibid.* **43** (1964) 202–210.
9. D. F. MOORE, in "Principles and applications of tribology" (Pergamon Press, New York, 1975) pp. 148–150.
10. Y. OSHIDA and T. NAKAYAMA, *J. Jpn Inst. Metals* **35** (1971) 1108–1114.
11. R. F. GOULD (ed.), "Contact angle: wettability and adhesion", *Adv. Chem. Ser.* **43** (1964).
12. I. NITTA, "X-ray crystallography" (Maruzen Publ., 1969).
13. M. L. WHITE, *J. Phys. Chem.* **68** (1964) 3083.
14. K. W. BEWIG and W. A. ZISMAN, *ibid.* **69** (1965) 4238.
15. J. W. TAYLOR, *Metallurgica* **50** (1954) 161.
16. S. W. STRAUSS, *Nucl. Sci. Engng* **8** (1960) 362.
17. A. V. GROSSE, *J. Inorg. Nucl. Chem.* (1964) 1349.